long and weak bonds, when compared to normal S-F single bonds, which have values ranging from about 1.53 to 1.56 Å (see Table V). These long S-F bonds in SF_4^-, combined with the above analysis of the electron spin density distribution, suggest the following idealized bonding scheme for SF_4^-. The four equatorial fluorines are bound to sulfur by two semi-ionic, three-center-four-electron bond pairs[40-43] involving the p_x and p_y orbitals of sulfur. The third p orbital of sulfur, the p_z orbital, accommodates primarily the unpaired free electron, while the remaining sulfur free valence electron pair is localized mainly in its s orbital.

For *trans*-SF_4O^-, the bonding of the four equatorial fluorines (calculated bond length = 1.77 - 0.04 = 1.73 Å) is similar to that proposed above for SF_4^-, i.e. weak, semi-ionic, three-center-four-electron bonds involving the sulfur p_x and p_y orbitals. The LDF calculated S—O bond length (1.464 - 0.04 = 1.42 Å) is comparable to normal S=O double bonds (r_{SO} in SF_4O = 1.406 Å),[34] supporting, for oxygen, a predominantly covalent bonding scheme through a sulfur sp_z hybrid, which also accommodates, to a large extent, the unpaired free electron. The bonding scheme in SF_4O^- is completed by the formation of an additional double bond between sulfur and oxygen.

In SF_5, the basic bonding scheme somewhat resembles that in *trans*-SF_4O^-, but the ionic character of the four equatorial bonds is less pronounced. This is not surprising in view of the lack of a formal negative charge (neutral radical versus radical anion) which strongly enhances semi-ionic bonding. This interpretation is nicely supported by the atomic charges calculated by the LDF method for these radicals. As predicted from the above analysis, the negative charges on the four equatorial fluorine ligands decrease from -0.431 in SF_4^- to -0.376 in *trans*-SF_4O^- to -0.212 in SF_5.

Conclusions

The novel SF_4^- and *trans*-SF_4O^- radical anions[44] were prepared by γ-irradiation of SF_5^- and SF_5O^- containing salts, respectively, and were characterized by their isotropic EPR spectra, which permitted the determination of the s-orbital electron spin densities. Although anisotropic EPR data were not available for a complete electron spin density analysis, the nature and bonding of these interesting radical anions were elucidated using local density functional calculations. LDF theory was also used to predict the geometries and vibrational spectra of these and other closely related radicals. The reliability of these calculations was confirmed by comparison with experimental data from several well-known sulfur fluorides and oxyfluorides.

Acknowledgment. The work at Rocketdyne was financially supported by both the U.S. Army Research Office and the Air Force Phillips Laboratories. The work at the University of Tennessee was supported by the Division of Chemical Sciences, Office of Basic Energy Sciences, U.S. Department of Energy (Grant #DE-FG05-88ER13852).

(40) Pimentel, G. C. *J. Chem. Phys.* **1951**, *19*, 446.
(41) Hach, R. J.; Rundle, R. E. *J. Am. Chem. Soc.* **1951**, *73*, 4321.
(42) Rundle, R. E. *J. Am. Chem. Soc.* **1963**, *85*, 112.
(43) Wiebenga, E. H.; Havinga, E. E.; Boswijk, K. H. *Adv. Inorg. Chem. Radiochem.* **1961**, *3*, 158.

(44) Morton and Preston have noted in ref 6 that for isoelectronic pairs of radicals the F^{19} hyperfine interaction is always larger in the radical anion than in the neutral species. The results of the present study are in accord with this generalization, since the F^{19} splittings for SF_4^- and SF_4O^- are greater than those for ClF_4 and SF_5, respectively (see Table I).

Motional Processes in Solid Organotin Polymers Investigated by One- and Two-Dimensional ^{13}C and ^{119}Sn NMR Spectroscopy

Jörg Kümmerlen and Angelika Sebald*

Contribution from the Bayerisches Geoinstitut, Universität Bayreuth, Postfach 10 12 51, W-8580 Bayreuth, Germany. *Received August 24, 1992*

Abstract: Variable-temperature one- and two-dimensional ^{13}C CP/MAS spectroscopy of a series of six crystalline trimethyltin compounds has demonstrated that the rate of Me_3Sn reorientation is significant on the NMR time scale. The combination of line shape analyses of the exchange-broadened ^{13}C CP/MAS spectra with rates obtained from 2D exchange spectra yields activation energies in the range of 38.6-72.5 kJ mol^{-1} for this series of compounds. Comparison of our NMR results with information from X-ray diffraction measurements leads us to postulate a $2\pi/3$ propeller-like jump around the tin-oxygen or tin-nitrogen bond, respectively, as the reorientation mechanism. Rotor-synchronized ^{119}Sn 2D magnetization-transfer experiments strongly support this view and indicate a rigid backbone for these chainlike polymers.

Introduction

Nuclear magnetic resonance (NMR) spectroscopy has proved to be a powerful tool for the elucidation of various types of molecular nonrigidity and fluxional behavior of organometallic complexes and molecules, both in solution and in the solid state.[1-3] Coherent averaging of anisotropic spin interactions by magic angle spinning (MAS), in combination with high power proton decoupling and cross-polarization (CP) techniques, enables the adoption of a variety of solution-state NMR techniques for the investigation of dynamic processes in solids, exploiting the properties of heteronuclei like ^{13}C or others. In line with the development of high-resolution solid-state NMR spectroscopy, experimental methods for the investigation of such processes have become available, ranging from wide line and relaxation measurements on abundant nuclei to magnetization-transfer experiments in one, two, and three dimensions.[4,5] This wide range of experimental

(1) Andrew, E. R.; Eades, R. G. *Proc. Roy. Soc. London* **1953**, *A218*, 537-552.
(2) Andrew, E. R. *J. Chem. Phys.* **1950**, *18*, 607-618.
(3) Sandström, J. *Dynamic NMR Spectroscopy*; Academic Press: London and New York, 1982.
(4) Blümich, B.; Spiess, H. W. *Angew. Chem.* **1988**, *100*, 1716-1734; *Angew. Chem., Int. Ed. Engl.* **1988**, *27*, 1655.
(5) Spiess, H. W. *Chem. Rev.* **1991**, *91*, 1321-1338.

0002-7863/93/1515-1134$04.00/0

Scheme I

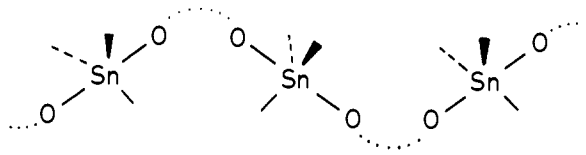

methods makes an equally wide range of rate constants accessible: variable-temperature solid-state NMR experiments on static or rotating samples are a powerful means of elucidating rate constants for molecular reorientation processes, either by comparison with simulated spectra or from the analysis of line width changes in the coalescence regime. While a considerable number of variable-temperature deuteron NMR studies have been published,[5,6] only a few examples can be found in the literature where detailed line shape analyses of variable-temperature CP/MAS spectra of other nuclei form the basis for the evaluation of rate constants or of mechanisms of dynamic processes in solid compounds.[7-9] Until recently, most of these studies have been performed on transition-metal complexes[7-10] where various reorientation modes of organic ligands, such as cyclopentadienyl groups, were established or on organic polymers.[4,5]

Here we report a CP/MAS NMR study (^{13}C, ^{119}Sn) on a series of five solid Me_3Sn-containing, crystalline organotin polymers and on one monomeric molecule, in all of which the Me_3Sn moieties display dynamic features in the solid state. For most of the compounds **1–6**, the ^{13}C CP/MAS spectra are strongly temperature-dependent in the temperature range of 200–383 K. The following six compounds have been investigated: **1**, $^tBu_2P$–NSN–$SnMe_3$; **2**, $Me_3SnN(SO_2Me)_2$; **3**, $Me_3SnN(SO_2Me)_2{\cdot}2H_2O$; **4**, $Me_3SnN(SO_2Me)_2{\cdot}Me_3SnOH$; **5**, $Me_3Sn(O_2CMe)$; and **6**, $(Me_3Sn)_2CO_3$.

Polymeric zigzag chains are very common structural units in the solid state for compounds of the type R_3SnX, depending on the steric and electronic requirements of the substituents R and X.[11,12] All our compounds **2–6** belong to this category as is evident from the single-crystal X-ray structures of these compounds (**2**,[13] **3**,[14] **4**,[15] **5**,[16] **6**[17]). The general structural unit of these polymers is a trigonal bipyramidal Me_3Sn arrangement which is axially bridged by oxygen-containing organic or inorganic units, as depicted in Scheme I. In all compounds **2–6** the oxygen–tin–oxygen bond angles are close to 180°, allowing assignment of the components of the axially symmetric (or nearly axially symmetric) ^{119}Sn shielding tensors: the $\sigma_\parallel$ component can be assumed to be approximately parallel to the O···Sn···O bond.

For none of the compounds **2–6** have the X-ray crystal structure determinations revealed any indication of molecular motion. This finding leads us to postulate a 3-site propeller-like $2\pi/3$ jump process of the Me_3Sn methyl groups around the O···Sn···O axis. Such a process will leave the X-ray diffraction results unaffected while other conceivable reorientational processes, like, e.g., diffusive motion of the individual methyl groups or of the entire Me_3Sn unit around their respective equilibrium positions, would certainly be detectable by X-ray diffraction techniques. All ^{13}C 1D and 2D CP/MAS spectra of **1–6**, which will be discussed in the following, have been analyzed assuming this propeller-like $2\pi/3$ jump mechanism of the Me_3Sn groups.

While it is most instructive to compare activation energies of reorientational processes in molecular nonassociated solid organometallic complexes to those found in solutions of such complexes, such a comparison is rather irrelevant in our case since the polymeric structure of these organotin compounds is not retained in solution. The activation energy for a reorientational process around the Me_3Sn–C_3 (or pseudo-C_3) axis in solution will usually be very low.

Experimental Section

Compounds **1–6** were synthesized and purified following published methods.[13-17,18] All NMR spectra were obtained on a Bruker MSL 300 NMR spectrometer equipped with Bruker double-bearing CP/MAS probes, an ASPECT 3000 computer, and a Bruker B-VT 1000 temperature control unit. Air-sensitive compounds **1** and **2** were packed in airtight Kel-F inserts[19] which fit exactly inside the standard 7-mm ZrO_2 rotors. Isotropic chemical shifts for ^{13}C (75.5 MHz) and ^{119}Sn (111.9 MHz) are given with respect to external Me_4Si (^{13}C) and external Me_4Sn (^{119}Sn), respectively. The ^{13}C and ^{119}Sn Hartmann–Hahn cross-polarization match was set on adamantane (^{13}C) and on tetracyclohexyltin (^{119}Sn) using a ^1H $\pi/2$ pulse length of 5 μs. Cross-polarization contact times for ^{13}C and ^{119}Sn between 0.75 and 8 ms were used; the contact times were optimized for each individual compound. Relaxation delays of 1–10 s were necessary, and spinning rates of 2.1–4.7 kHz were used. For variable-temperature work, dry nitrogen served as both driving and bearing gas. Thermal equilibration of the samples at each temperature was typically reached after 20 min. For rotor-synchronized ^{119}Sn 2D exchange experiments, synchronization of the pulse programmer with the rotor position was achieved by using a homebuilt "synchro-spin" apparatus which has been described elsewhere.[20] The principal components of the ^{119}Sn chemical shift tensors were obtained by iterative simulation of the respective spinning sideband patterns on the basis of the moment analysis by Maricq and Waugh.[21]

Methodology

Consideration of typical room temperature ^{13}C and ^{119}Sn CP/MAS spectra of compounds **1–6** reveals the necessity to take different time regimes into account, both with respect to exchange rates and with respect to chemical shift anisotropies. These different regimes determine the experimental methodology necessary for the extraction of the desired kinetic information. Before discussing our results, we will, therefore, digress briefly into such methodology aspects.

With the exception of **2** and **5**, all compounds **1–6** show fairly broad Me_3Sn–^{13}C resonances near room temperature. Such exchange-broadened resonances make the use of one-dimensional variable-temperature ^{13}C CP/MAS spectroscopy accessible for the determination of jump rates (and activation energies). Furthermore, with MAS spinning frequencies of 3.5–4.2 kHz, these methyl resonances may be treated as isotropic lines given that the shielding anisotropy is spun out. Therefore, on the basis of variable-temperature ^{13}C CP/MAS spectra, dynamic processes concerning the Me_3Sn unit may be described within the framework of classical multisite exchange theory. In the specific case of a three-site exchange problem, the situation is simplified by the fact that there is no difference between nearest-neighbor and all-site exchange. As has been shown by Spiess[22] and Mehring,[23] the complex line shape function for a N-site exchange problem may be written in a simple and compact form if T_2 processes are ignored

$$g(\omega) = \frac{1}{N}\frac{1}{1-\kappa L} \qquad (1)$$

$$L = \sum_{j=1}^{N}[i(\omega - \omega j) + N\kappa]^{-1}$$

(6) See for example: Fyfe, C. A. *Solid State NMR for Chemists*; C.F.C. Press: Ontario, 1983; and references given therein.
(7) Heyes, S. J.; Dobson, C. M. *J. Am. Chem. Soc.* **1991**, *113*, 463–469.
(8) Heyes, S. J.; Green, M. L. H.; Dobson, C. M. *Inorg. Chem.* **1991**, *30*, 1930–1937.
(9) Heyes, S. J.; Gallop, M. A.; Johnson, B. F. G.; Lewis, J.; Dobson, C. M. *Inorg. Chem.* **1991**, *30*, 3850–3856.
(10) Spiess, H. W.; Grosescu, R.; Haeberlen, K. *Chem. Phys.* **1974**, *6*, 226–234.
(11) Molloy, K. C. In Chemistry of Tin; Harrison, P. G., Ed.; Blackie: Glasgow and London, 1989; pp 187–220.
(12) Tiekink, E. R. T. *Appl. Organomet. Chem.* **1991**, *5*, 1–23.
(13) Blaschette, A.; Schomburg, D.; Wieland, E. *Z. Anorg. Allg. Chem.* **1988**, *566*, 103–110.
(14) Blaschette, A.; Schomburg, D.; Wieland, E. *Z. Anorg. Allg. Chem.* **1989**, *571*, 75–81.
(15) Blaschette, A.; Wieland, E.; Jones, P. G.; Hippel, I. *J. Organomet. Chem.*, in press.
(16) Chih, H.; Penfold, B. R. *J. Cryst. Mol. Struct.* **1973**, *3*, 285–297.
(17) Kümmerlen, J.; Sebald, A.; Reuter, H. *J. Organomet. Chem.* **1992**, *427*, 309–323.
(18) Frank, S. Ph.D. Thesis, University of Bayreuth, 1990.
(19) Merwin, L. H.; Sebald, A.; Espidel, J. E.; Harris, R. K. *J. Magn. Reson.* **1989**, *84*, 367–371.
(20) Kümmerlen, J.; Sebald, A.; Weigel, R. *Solid State NMR* **1992**, *7*, 231–234.
(21) Maricq, M. M.; Waugh, J. S. *J. Chem. Phys.* **1979**, *70*, 3300–3316.
(22) Spiess, H. W. In *NMR—Basic Principles and Progress*; Diehl, P.; Fluck, E.; Kosfeld, R., Eds.; Springer Verlag: Berlin, 1978; Vol. 15, pp 59–214.
(23) Mehring, M. *Principles of High Resolution NMR in Solids*; Springer Verlag: Berlin, 1983; pp 8–62.

With $N = 3$ the spectrum $I(\omega) = \mathrm{Re}\{g(\omega)\}$ may be expressed as

$$I(\omega) = \frac{2\kappa\Omega_2(\Omega_2 - 27\kappa^2) - 18\kappa(\omega - \langle\omega\rangle)[\Omega_3 - 9\kappa^2(\omega - \langle\omega\rangle)]}{4\kappa^2\Omega_2^2 + [\Omega_3 - 9\kappa^2(\omega - \langle\omega\rangle)]^2} \quad (2)$$

where

$$\kappa = \text{jump rate}$$

$$\langle\omega\rangle = {}^1/_3(\omega_1 + \omega_2 + \omega_3)$$

$$\Omega_2 = (\omega - \omega_1)(\omega - \omega_2) + (\omega - \omega_1)(\omega - \omega_3) + (\omega - \omega_2)(\omega - \omega_3)$$

$$\Omega_3 = (\omega - \omega_1)(\omega - \omega_2)(\omega - \omega_3)$$

A simulation program based on eq 2 was written to evaluate the jump rates κ at different temperatures from the experimental variable-temperature ^{13}C CP/MAS spectra. ^{13}C CP/MAS spectra were recorded at temperatures between 200 and 300 K. In general, spectra of compounds **1** and **3–6** obtained at 220 and 200 K were identical with respect to line shape and line width at half-height. The line widths from these spectra were taken as the natural line widths (typically ca. 15 Hz). In the fitting procedure, this line width was taken into account by convoluting each calculated spectrum with a Lorentzian prior to comparison with the experimental spectra.

Clearly, the applicability of variable-temperature one-dimensional ^{13}C CP/MAS spectroscopy for such purposes is limited by the experimentally accessible temperatures and by the thermal stability of the compounds under investigation; sufficiently well-resolved spectra for the different sites in the slow-exchange regime are required. Two-dimensional (2D) ^{13}C magnetization-transfer experiments are then the method of choice to obtain exchange rates for those cases where the exchange-broadened regime is not accessible by temperature variation (e.g., compounds **2** and **5**). In addition, 2D ^{13}C exchange spectroscopy extends the range of available jump rates also for those cases where variable temperature 1D ^{13}C CP/MAS spectroscopy *is* feasible: data for the slow-exchange regime, where line shape analysis is no longer informative, become available and thus improve the quality of the data set used for the calculation of activation energies (Arrhenius plot).

The 2D ^{13}C magnetization-transfer experiments were recorded using the pulse sequence[24] CP-t_1-$\pi/2$-τ_m-$\pi/2$-t_2 with quadrature detection (TPPI method[25]) in the t_1 dimension. Typically, mixing times τ_m between 50 ms and 1.2 s were used. Symmetrization of the spectra was not necessary. In order to discriminate between exchange processes and proton-mediated spin diffusion effects, in each case an experiment with $\tau_m = 200$ ms with and without high-power proton decoupling during τ_m was performed. The intensity ratio I_o/I_d (I_o, intensity of the off-diagonal peaks; I_d, intensity of the diagonal peaks) was the same, within experimental error, for both types of experiment. Spin diffusion processes can therefore be excluded as a source of the off-diagonal peaks. Rate constants were obtained using eq 3 on the basis of the initial rate approximation[26]

$$\kappa_{kl} = \frac{S_{kl}}{S_0 \cdot \tau_m} \quad (3)$$

$$\tau_m = \text{mixing time}$$

$$S_{kl} = \text{off-diagonal signal intensity}$$

$$S_0 = \text{diagonal intensity for } \tau_m = 0\text{s}$$

Magnetization losses via T_1 processes during the mixing time τ_m were found to be negligible.

Finally, the ^{119}Sn nuclei in **1–6** provide an additional probe for further investigations of the observed dynamic processes, this time addressing questions concerning the rigidity of the polymeric backbone. Unlike the Me_3Sn–^{13}C resonances, the ^{119}Sn spectra of **1–6** belong to the category of high field/slow spinning CP/MAS spectra, i.e., the ^{119}Sn chemical shift anisotropies $\Delta\sigma$ are much greater than the MAS spinning rates of 3–4 kHz. Within this slow spinning regime, conventional (i.e., nonrotor-synchronized) 2D exchange spectroscopy will always give rise to off-diagonal peaks between spinning sideband manifolds, even in the absence of motion and spin diffusion. Of course, 2D exchange experiments on static samples will not suffer from this problem and, indeed, have been widely used, monitoring nuclei like, e.g., ^2D, ^{13}C, and ^{31}P.[4,27-29]

Table I. ^{119}Sn NMR Parameters for Compounds **1–6**[a]

compound	$\delta^{119}Sn$ (ppm)	σ_{11}	σ_{22}	σ_{33}	η
1, $^tBu_2P$–NSN–$SnMe_3$[b]	46.2	13	−35	−117	0.7
2, $Me_3SnN(SO_2Me)_2$	73.6	63	25	−310	0.2
3, $Me_3SnN(SO_2Me)_2 \cdot 2H_2O$	37.2	105	77	−294	0.1
4, $Me_3SnN(SO_2Me)_2 \cdot Me_3SnOH$	94.8	26	−53	−258	0.5
	68.6	44	1	−251	0.2
5, $Me_3Sn(O_2CMe)$	−27.2	183	158	−259	0.1
6, $(Me_3Sn)_2CO_3$[c]	123.5	−188	−138	−44	0.6
	−62.0	246	192	−252	0.2

[a] Tensor parameters are given following Haeberlen's notation with $-\delta_{iso} = \sigma_{iso} = {}^1/_3(\sigma_{11} + \sigma_{22} + \sigma_{33})$; $|\sigma_{33} - \sigma_{iso}| \geq |\sigma_{11} - \sigma_{iso}| \geq |\sigma_{22} - \sigma_{iso}|$; $\delta_A = \sigma_{33} - \sigma_{iso}$; $\Delta\sigma = {}^3/_2\delta_A$; $\eta = {}^2/_3(\sigma_{22} - \sigma_{11})(\Delta\sigma)^{-1}$. [b] $^1J(^{119}Sn^{14}N) = 105 \pm 5$ Hz; $\delta^{31}P = +81.7$ with $\nu_{1/2} = 110$ Hz at $T = 203$ K. [c] Data taken from ref 17.

Table II. ^{13}C NMR Parameters for Compounds **1–6**

compd	T (K)	$\delta^{13}C$ (Me_3Sn) (ppm)[a]	remaining $\delta^{13}C$ (ppm)
1	213	−3.1; −1.4; +2.2	35.1; 27.9 (^tBu)
2	297	4.0; 3.4; 2.9	44.5; 43.6 ($N(SO_2Me)_2$)
3	210	0.7; −0.8 relative intensity 2:1	45.1; 44.4 ($N(SO_2Me)_2$)
4	210	4.5; 2.5; 0.0 4.1; 2.7; −1.2	44.3; 43.1 ($N(SO_2Me)_2$)
5	297	1.3; −0.5 relative intensity 2:1	25.3; 178.6 (O_2CMe)
6[b]	297	2.2; 0.7; −0.7 approx −1 (broad)	163.8 (CO_3)

[a] $^1J(^{119/117}Sn^{13}C)$, where identified, is in the range of 440–525 Hz. [b] Data taken from ref 17.

In our case, static ^{119}Sn 2D exchange experiments are not particularly promising, given sensitivity problems (not even to mention inherent problems of static CP spectra) and overlapping ^{119}Sn csa tensor patterns in samples **4** and **6**.

De Jong et al.[30,31] have proposed an experimentally easy to perform 2D exchange experiment for the slow spinning regime: if the mixing time τ_m is an integral multiple of the rotor period, any off-diagonal intensity in the 2D exchange spectra will be solely due to motion (or spin diffusion). Further practical[20] and theoretical[31,32] details, including the specific phase cycling required for the selection of the coherence antiecho component, have been discussed elsewhere. We followed the approach of de Jong et al.,[30,31] and our rotor-synchronized ^{119}Sn 2D exchange spectra are represented in the magnitude mode. Clearly, pure absorption mode representation is, in general, superior to the magnitude representation, and Spiess and co-workers have outlined an elegant method to obtain spectra in this way.[28] However, for the purposes of our investigation, i.e., strictly qualitative use of the ^{119}Sn 2D exchange spectra, the magnitude representation was satisfactory, given that no severe overlap problems on the diagonal of the 2D matrix were encountered.

Results

Representative one- and two-dimensional ^{13}C and ^{119}Sn CP/MAS spectra of **1–6** are depicted in Figures 1–10. Tables I–III summarize the NMR data for **1–6** as well as the respective activation energies E_a for the $2\pi/3$ propeller-like jump processes. In this section the NMR results are outlined in conjunction with the more prominent findings from X-ray diffraction for **2–6**. In the following section we will then present a somewhat more generalized discussion of the results.

Compound 1, $^tBu_2PNSNSnMe_3$. Of all compounds **1–6**, $^tBu_2PNSNSnMe_3$ is the only one for which no single crystal X-ray structure determination has been carried out due to the lack of suitable single crystals. Generally speaking, disubstituted sul-

(24) Ernst, R. R.; Bodenhausen, G.; Wokaun, A. *Principles of Nuclear Magnetic Resonance in One and Two Dimensions*; Oxford Science Publ.: Oxford, U.K., 1991; pp 490–538.
(25) See ref 24; p 496.
(26) See ref 24; pp 495–501.
(27) Schaefer, D.; Spiess, H. W.; Suter, K. W.; Fleming, W. W. *Macromolecules* **1990**, *23*, 3431–3439.
(28) Hagemeyer, A.; Schmidt-Rohr, K.; Spiess, H. W. *Adv. Magn. Reson.* **1989**, *13*, 85–130.
(29) Fenske, D. B.; Jarrell, H. C. *Biophys. J.* **1991**, *59*, 56–69.
(30) de Jong, A. F.; Kentgens, A. P. M.; Veeman, W. S. *Chem. Phys. Lett.* **1984**, *109*, 337–342.
(31) Kentgens, A. P. M.; de Boer, E.; Veeman, W. S. *J. Chem. Phys.* **1987**, *87*, 6859–6866.
(32) Geen, H.; Bodenhausen, G. *J. Chem. Phys.* **1992**, *97*, 2928–2937.

Table III. Activation Energies for $2\pi/3$ Me_3Sn Reorientation for Compounds **1–5**

compound	1	2	3	4	5
activation energy (kJ mol^{-1})	49.4 ± 6.9	72.5 ± 4.2	43.9 ± 4.0	38.6 ± 3.0 44.8 ± 3.0	68.5 ± 6.1

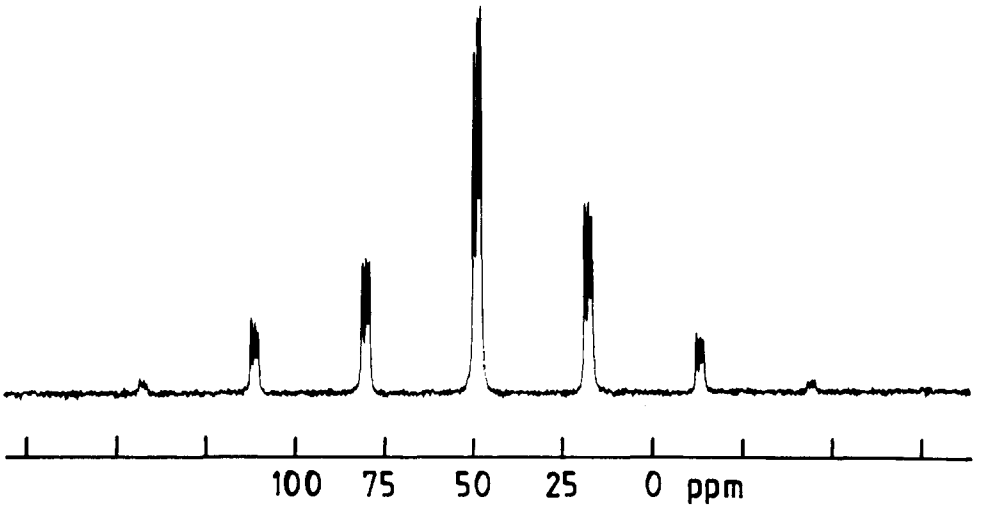

Figure 1. ^{119}Sn CP/MAS spectrum of **1** at room temperature, ν_{rot} = 3464 Hz, 848 transients.

furdiimides RNSNR′ display a high degree of fluxionality in solution at ambient temperature, including rapid interconversion of different *E* and *Z* configurations.[18,33] Figure 1 shows the room temperature ^{119}Sn CP/MAS spectrum of **1**, displaying one ^{119}Sn resonance with an isotropic ^{119}Sn chemical shift of 46.2 ppm, moderate chemical shift anisotropy and further fine structure of the center band and of all spinning sidebands. This further splitting is due to scalar coupling $^1J(^{119}Sn^{14}N)$ = 105 ± 5 Hz, representing, within experimental error, a case where no residual dipolar coupling ^{14}N–^{119}Sn is observed in the ^{119}Sn CP/MAS spectrum (see Figure 1). Comparison of the ^{119}Sn CP/MAS spectrum of **1** with variable-temperature solution-state NMR spectra of **1** and of several similar compounds[18,33] is consistent with the presence of only one configurational isomer in the solid state at room temperature; the most likely solid-state configuration is given by

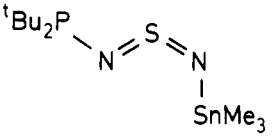

No changes of the ^{119}Sn CP/MAS spectrum of **1** as a function of temperature in the temperature range of 193–293 K were observed. Therefore, configurational isomerization of solid **1** can be excluded. In contrast to this, the Me_3Sn region in the ^{13}C CP/MAS spectrum of **1** is strongly temperature-dependent in the range of 273–292 K, as may be seen in Figure 2. It should be mentioned that the *tert*-butyl region in the ^{13}C CP/MAS spectra of **1** (not shown) is also strongly temperature-dependent in the 183–293 K range. Whatever the exact nature of this latter process involving the $^tBu_2P$ group in **1**, it is seemingly unrelated to the $2\pi/3$ jump of the Me_3Sn group around the Sn–N bond and will not be discussed further here. Certainly further work focused on the dynamic properties of disubstituted solid sulfurdiimides will have to address this question as well; here we will concentrate our attention to the properties of the Me_3Sn group. Figure 2 shows typical experimental variable-temperature ^{13}C CP/MAS results for **1** along with the respective simulated spectra, assuming a $2\pi/3$ jump. For example, the spectrum at 280 K corresponds to a jump rate $\kappa = 20\ s^{-1}$. Combining the results from eight one-dimensional variable-temperature ^{13}C CP/MAS spectra and from three 2D exchange experiments yields the activation energy for this process E_a = 49.4 ± 6.9 kJ mol^{-1}.

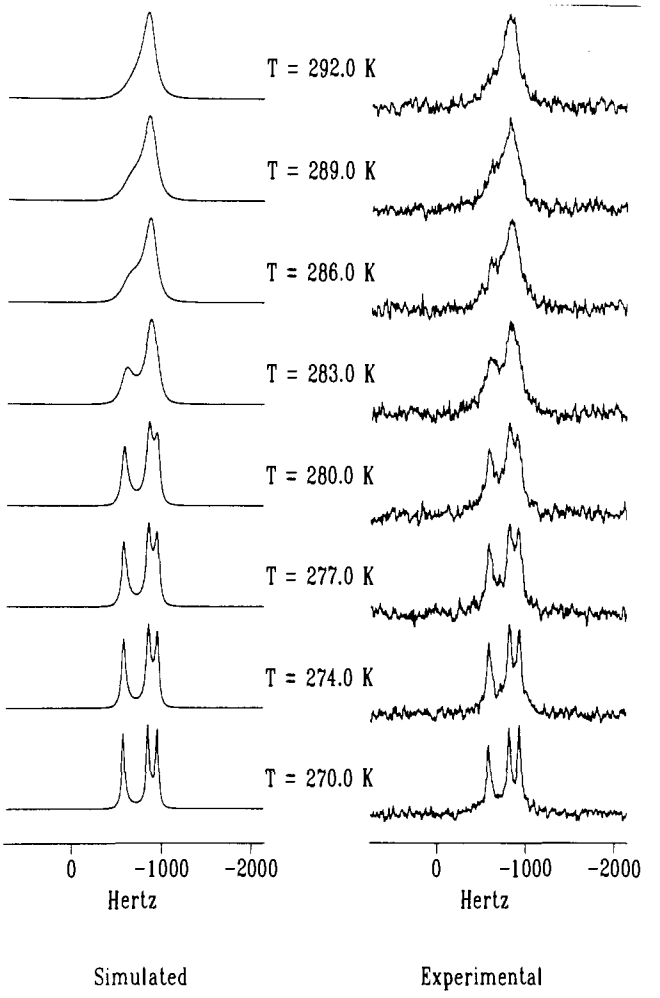

Figure 2. Experimental (right) and simulated (left) ^{13}C CP/MAS spectra of **1** in the exchange-broadened temperature range 270–292 K. Only the Me_3Sn region is shown. Typically ν_{rot} = 2.7 kHz, 160 transients.

(33) Herberhold, M.; Gerstmann, S.; Wrackmeyer, B. *Phosphorus, Sulfur, Silicon Relat. Elem.* **1992**, *66*, 273–283.

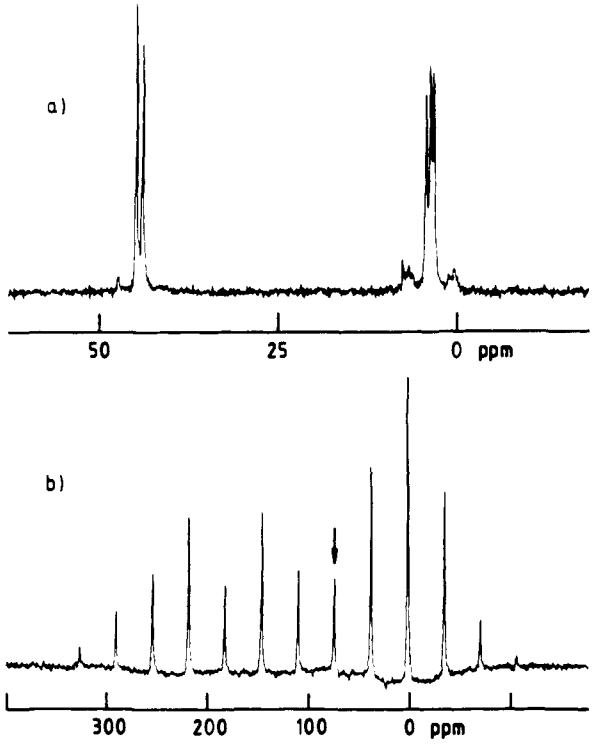

Figure 3. (a) ^{13}C CP/MAS spectrum of **2** at room temperature, ν_{rot} = 2816 Hz, 414 transients. (b) ^{119}Sn CP/MAS spectrum of **2** at room temperature, ν_{rot} = 4030 Hz, 2352 transients.

Compound 2, $Me_3SnN(SO_2Me)_2$. Solid **2** forms infinite zigzag chains parallel to the crystallographic *a* axis,[13] the Me_3Sn units being bridged by the bidentate $N(SO_2Me)_2$ ligands. While there

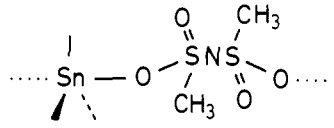

is only one crystallographically unique tin site in the asymmetric unit, the three methyl carbon atoms of the Me_3Sn group are crystallographically inequivalent. In agreement with the X-ray crystallographic structure, the room temperature ^{119}Sn CP/MAS spectrum of **2** shows one resonance (73.7 ppm, see Figure 3a) and an almost axially symmetric csa tensor pattern with an asymmetry parameter η = 0.16. The room temperature ^{13}C CP/MAS spectrum of **2** (see Figure 3b) shows three resolved resonances for the three crystallographically inequivalent Me_3Sn carbon atoms (4.0, 3.4, 2.9 ppm). Temperature variation in the range of 243–333 K does not affect the shape or line width of these three Me_3Sn ^{13}C resonances ($\nu_{1/2}$ = 15 Hz). 2D ^{13}C magnetization-transfer experiments, however, show that mutual exchange between the three methyl positions occurs at room temperature with a rate κ = 2.1 s^{-1}. The contour plot in Figure 4 depicts a typical ^{13}C 2D exchange experiment on **2** at T = 313 K, using a mixing time of 100 ms. Using rate constants for the $2\pi/3$ propeller-like jump from nine experiments (at six different temperatures), we can calculate the activation energy E_a = 72.5 ± 4.2 kJ mol^{-1}. This is the highest activation energy observed within our series of polymeric compounds **2–6**. Compound **2** also shows the most expressed deviation from a regular trigonal bipyramidal Me_3SnO_2 environment within this series: while the O–Sn–O bond angle of 172.9 (7)° and the O–Sn bond lengths 227.5 (24) and 230.1 (39) pm for **2** are fairly similar to the average values found for this type of polymer (average O–Sn–O bond angle ≈173.7°, average O–Sn bond length 228.2 pm, the O–Sn–C_{methyl} bond angles for **2** vary from 66.4 (16)° to 116.1 (14)°.[13] In other words, the plane defined by the three methyl carbon atoms of the Me_3Sn moiety in **2** is not quite perpendicular to the O–Sn–O axis.

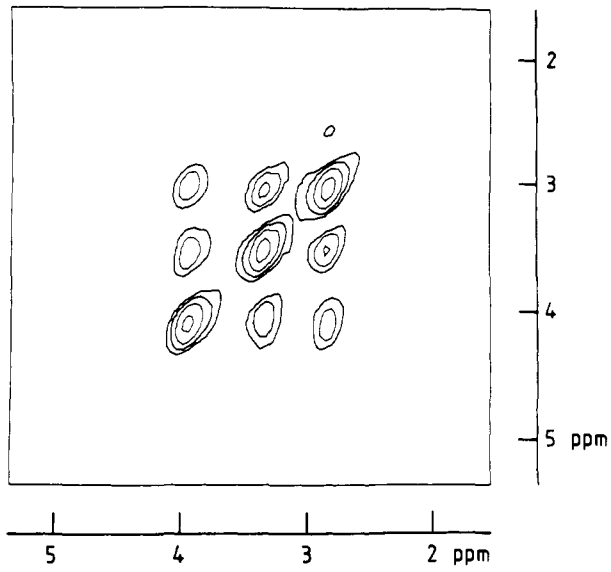

Figure 4. ^{13}C 2D magnetization-transfer experiment on **2** at T = 312 K, mixing time τ_m = 100 ms. Only the Me_3Sn region is shown. ν_{rot} = 2890 Hz, 64 transients. TD1 = 128 W, TD2 = 256 W; zero-filled to 512 W in both dimensions before processing, no symmetrization.

Compound 3, $Me_3SnN(SO_2Me)_2 \cdot 2H_2O$. Compound **3** also forms infinite chains in the solid state. These chains may be viewed as composed of diaquatrimethyltin cations, linked by dimesylaminide anions via hydrogen bonds. The asymmetric unit contains four

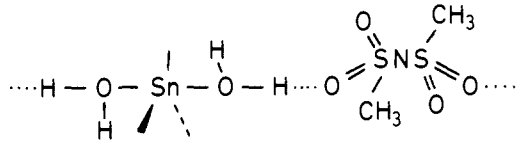

crystallographically equivalent cation/anion pairs. The tin atom is located in the center of an only slightly distorted trigonal bipyramid.[14] The O–Sn bond lengths (232.7 and 225.4 pm) do not deviate much from the average value for symmetric O–Sn–O arrangements. The O–Sn–O bond angle of 177.0 (1)° is only slightly smaller than the ideal 180° angle, and the O–Sn–C_{methyl} bond angles range from 86.9 (1)° to 90.8 (1)°. This results in a structure for **3** in which the Me_3Sn carbons define a plane almost perpendicular to the O–Sn–O axis of rotation, i.e., to the $2\pi/3$ jump axis. In line with these X-ray crystallographic findings one ^{119}Sn resonance (37.3 ppm), displaying a csa tensor pattern close to axial symmetry (η = 0.1), is found in the ^{119}Sn CP/MAS spectrum of **3**. The three Me_3Sn methyl groups in **3** are crystallographically inequivalent, and the low-temperature limit ^{13}C CP/MAS spectrum of **3** (T = 210 K) exhibits two resonances for the methyl carbon atoms at 0.7 and −0.8 ppm in a 2:1 intensity ratio.

Increasing the temperature above 270 K leads to typical exchange-broadened ^{13}C CP/MAS spectra of **3**; above 310 K only one resonance at 0.6 ppm remains in the fast exchange regime for the three-site $2\pi/3$ jump exchange. Jump rates have been determined from spectra obtained in the 273–301 K temperature range. Experimental and simulated ^{13}C CP/MAS spectra for **3** are shown in Figure 5. In addition, 2D ^{13}C magnetization-transfer experiments at temperatures below 270 K have been performed. The combined set of kinetic data from both series of experiments shows the expected Arrhenius-type behavior, and the activation energy for the 3-site jump in solid **3** is E_a = 43.9 ± 4.0 kJ mol^{-1}.

Compound 4, $Me_3SnN(SO_2Me)_2 \cdot Me_3SnOH$. For solid **4**, X-ray crystallography finds two independent Me_3Sn units, connected by an OH bridge in such a way that the two units share the OH oxygen atom as one apex of their respective trigonal bipyramidal coordination. One oxygen atom of the bidentate dimesylaminide anion then provides the second apex of the bipyramid. While the Sn^1–O(H) (211.8 pm) and Sn^2–O(H) (212.6 pm) distances are

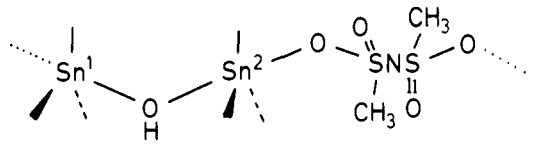

slightly shorter than the average Sn–O distance found for this class of polymers, the Sn^1,Sn^2–O bond lengths 268.2 and 253.3 pm are significantly larger than this average value. The O–$Sn^{1,2}$–O(H) bond angles 174.5 (1)° and 173.8 (1)° are very similar and reasonably close to proper axial symmetry. Keeping the large differences in bond lengths $Sn^{1,2}$–O(H) vs $Sn^{1,2}$–O in **4** in mind, this compound should be viewed as an infinite chain in which $(Me_3Sn)_2OH$ cations are linked by dimesylaminide anions. The ^{119}Sn CP/MAS spectrum of **4** consists of two resonances at 94.8 and 68.6 ppm, respectively, reflecting the two different tin environments. The room temperature ^{13}C CP/MAS spectrum of **4** shows two sharp resonances for the methyl carbon atoms of the dimesylaminide "spacer" (44.3 and 43.1 ppm) and a broad unresolved resonance in the Me_3Sn–^{13}C chemical shift range. On decreasing the temperature, this broad resonance gradually becomes sharper and splits into six resolved resonances at temperatures below 240 K (see Figure 6).

Simply by inspection, these six resonances can be subdivided into a pair of three resonances each: the integrated intensities of the ^{13}C resonances are not quite equal for the two different Me_3Sn moieties, reflecting slightly different cross-polarization efficiencies and thus allowing assignment. Over the whole temperature range of 243–299 K where exchange broadening for the Me_3Sn ^{13}C resonances occurs, the two ^{13}C resonances for the dimesylaminide group remain sharp, and there are no changes with respect to isotropic chemical shift or line width as a function of temperature.

With respect to the Me_3Sn reorientation, variable-temperature ^{13}C CP/MAS spectra in the 243–299 K range have been analyzed (the results are depicted in Figure 6). This analysis did not take the slightly different CP efficiency for the two Me_3Sn groups into account. That using a 1:1 intensity ratio for the simulation (in this case) does not result in significant errors for the determination of the jump rates is verified by comparison of these results with those obtained from ^{13}C 2D magnetization-transfer experiments (see below).

Inspection of the variable-temperature ^{13}C CP/MAS spectra of **4** in Figure 6 also reveals that the activation energies for the rotational reorientation of the two different Me_3Sn groups in **4** must be slightly different. Not only does this help to assign the connectivities of these resonances but it must also be taken as a strong indication that these two reorientational processes take place independently of each other. Of course, ^{13}C 2D magnetization-transfer experiments also reveal the different jump rates of the two Me_3Sn groups: for any given set of experimental parameters within the limits of the initial rate approximation, strong off-diagonal peaks are present for one of the Me_3Sn groups while only slight off-diagonal intensity is observed for the other one. As an example, the ^{13}C 2D exchange spectrum of **4** at T = 220 K with τ_m = 500 ms is shown in Figure 7.

The combined kinetic data yield $2\pi/3$ jump activation energies for **4** of E_a = 38.6 ± 3 and 44.8 ± 3 kJ mol^{-1}, respectively.

Considering the rather short Sn^1–(OH)–Sn^2 bond distances in **4**, at this point we cannot safely exclude that ^{13}C spectroscopy in this case may monitor some reorientational process concerning the $(Me_3Sn)_2OH$ cation as a whole, even if the two different activation energies would render such a possibility rather unlikely. At this point the ^{119}Sn nuclei can be advantageously used for further confirmation of the proposed 3-site jump process. The proposed $2\pi/3$ jump process cannot result in any off-diagonal intensity in a rotor-synchronized ^{119}Sn 2D exchange experiment, because the relative orientation of the individual tensor components will not be affected. In contrast to this, a jump or diffusive process involving the $(Me_3Sn)_2OH$ unit as a whole would render the relative tensor orientations time-dependent and thus yield off-diagonal intensity in the rotor-synchronized ^{119}Sn 2D exchange

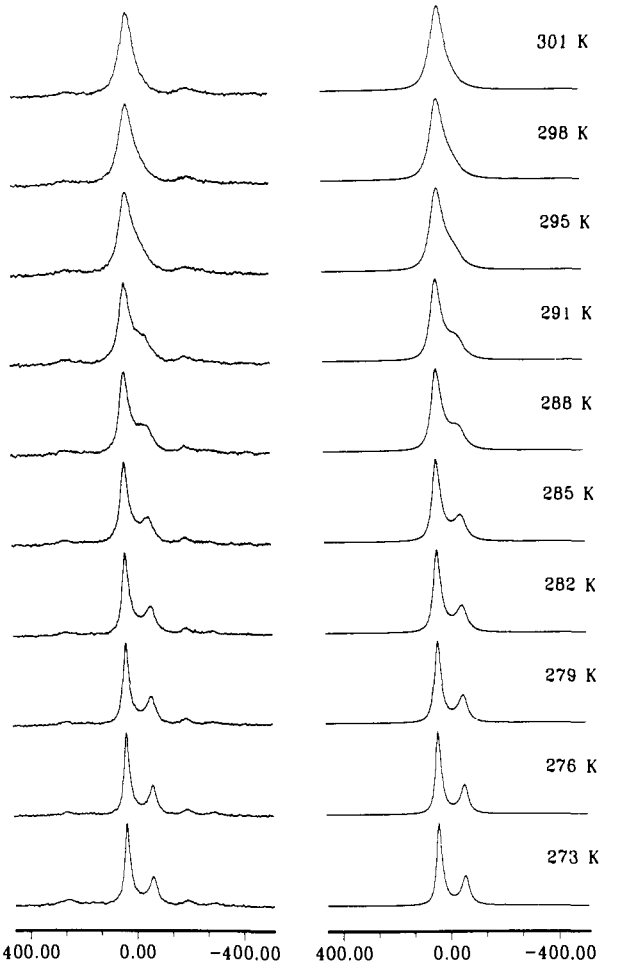

Figure 5. Experimental (left) and simulated (right) ^{13}C CP/MAS spectra of **3** in the temperature range of 273–310 K. Only the Me_3Sn region is shown. ν_{rot} = 3 kHz, 168 transients, bottom scales in Hz.

spectrum. It is obvious from Figure 8 that no significant off-diagonal intensity is observed, not even with mixing times of 20 s. The result is consistent with independent $2\pi/3$ jumps of the two individual Me_3Sn groups. It should, however, be mentioned that within the temperature range of 200–263 K, slight changes of $\delta^{119}Sn$ for **4** have been observed: while the high-frequency resonance gradually changes from 90.5 ppm at 200 K to 94.2 ppm at 263 K (0.06 ppm/K), the temperature effect on the lower-frequency ^{119}Sn resonance is more pronounced. This resonance shifts from 56.4 ppm (200 K) to 65.8 ppm (263 K), corresponding to a temperature shift of 0.15 ppm/K.

Obviously, polymeric solid Me_3SnOH would be a suitable model compound for comparison: in a sense also Me_3SnOH contains $(Me_3Sn)_2OH$ units such as in compound **4**. Such a comparison is, however, severely hampered due to the unknown X-ray crystal structure of Me_3SnOH. In the case of Me_3SnOH, NMR spectroscopy alone can only provide a few hints. Me_3SnOH shows a ^{119}Sn resonance at −99.0 ppm, with shielding tensor components σ_{11} = 257.4, σ_{22} = 254.5 and σ_{33} = −214.9 ppm, representing an axially symmetric case with η = 0.0 within the error of the tensor component determination. The resonance is substantially broader than what we usually observe for such (crystalline) Me_3SnO_2 arrangements ($\nu_{1/2}$ = 270 Hz). Possibly there are two unresolved ^{119}Sn resonances with a chemical shift difference of less than 2 ppm displaying very similar tensor components. Neither the shape of the ^{119}Sn csa tensor pattern nor the line width of the ^{119}Sn resonance of Me_3SnOH varies in the temperature range of 200–293 K. At ambient temperature, Me_3SnOH displays a broad and unresolved ^{13}C resonance. The shape of the ^{13}C resonance does not change significantly as a function of temperature within that range; not even the lowest accessible temperature (193 K) yielded sufficiently well-resolved resonances to allow further

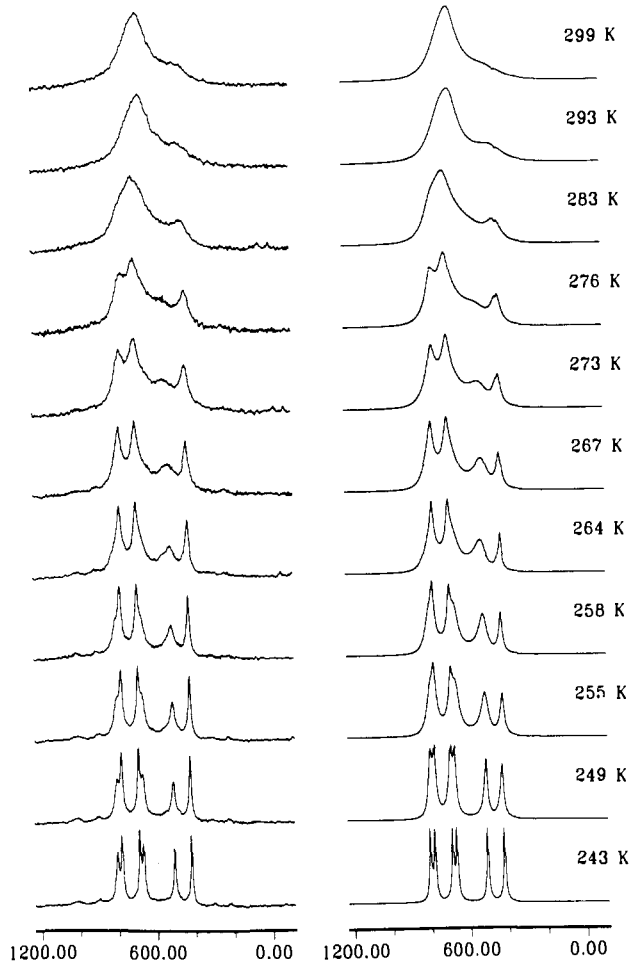

Figure 6. Experimental (left) and simulated (right) ^{13}C CP/MAS spectra of **4** in the temperature range of 243–299 K. Only the Me_3Sn region is shown. ν_{rot} = 4 kHz, 168 transients, bottom scales in Hz.

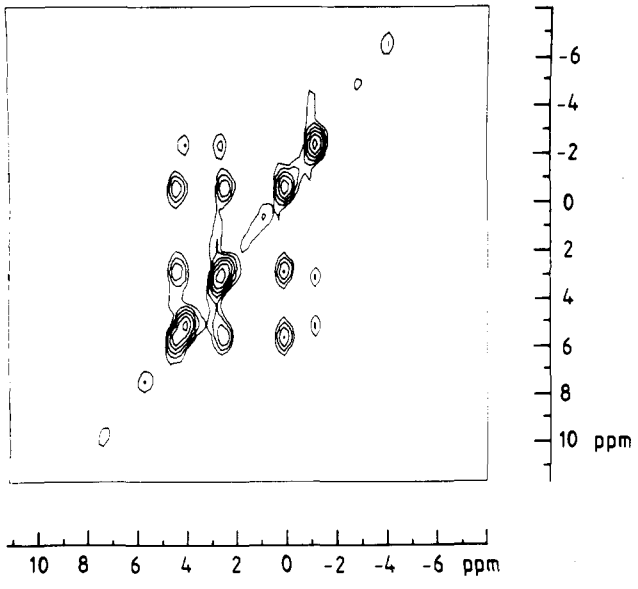

Figure 7. ^{13}C 2D magnetization-transfer experiment on **4** at T = 220 K, mixing time τ_m = 500 ms. Only the Me_3Sn region is shown. ν_{rot} = 2163 Hz, 16 transients. TD1 = 256 W, TD2 = 1 K; TD1 zero-filled to 1 K before processing, no symmetrization.

analysis. Selective one-dimensional ^{13}C excitation experiments (SELDOM, see below),[34] however, gave indications for the presence of a motional process in Me_3SnOH. Based on these observations for Me_3SnOH we can assume that (i) it is most likely that Me_3SnOH also undergoes a similar reorientational process with jump rates comparable to those for compounds **1–6** and (ii) the pertinent unresolved ^{13}C resonances for Me_3SnOH could be an indication of a rather complicated crystal structure of Me_3SnOH, comprising several inequivalent Me_3Sn moieties.

(34) Tekely, P.; Brondeau, J.; Elbayed, K.; Retournard, A.; Canet, D. *J. Magn. Reson.* **1988**, *80*, 509–516.

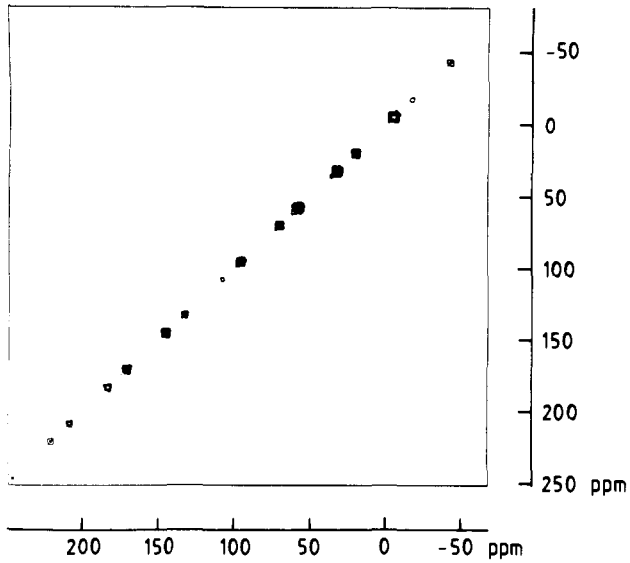

Figure 8. ^{119}Sn rotor-synchronized 2D exchange experiment on **4** at room temperature, ν_{rot} = 3268 Hz, mixing time τ_m = 20 s, 64 transients. TD1 = 128 W, TD2 = 1 K; TD1 zero-filled to 1 K before processing.

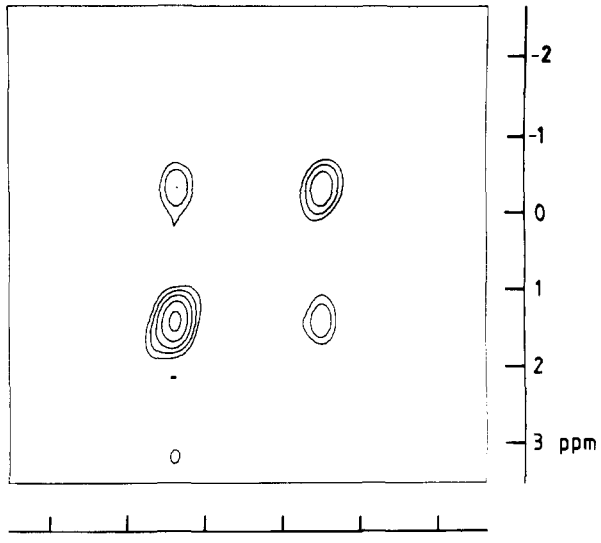

Figure 9. ^{13}C 2D magnetization-transfer experiment on **5** at T = 309 K, mixing time τ_m = 150 ms. Only the Me_3Sn region is shown. ν_{rot} = 3120 Hz, 48 transients. TD1 = 128 W, TD2 = 512 W; TD1 zero-filled to 512 W before processing, no symmetrization.

Compound 5, $Me_3Sn(O_2CMe)$. Like **2–4**, solid $Me_3Sn(O_2CMe)$ also belongs to the chain-building polymeric variety, except that now the chain-propagating bidentate ligand is a carboxylate anion.[16] Accordingly, the room temperature ^{119}Sn CP/MAS spectrum of **5** displays one ^{119}Sn resonance (−27.2 ppm) and a ^{119}Sn csa tensor pattern close to axial symmetry. The ^{13}C CP/MAS spectrum of **5** is unaffected by temperature variation from 243 to 333 K. Over this temperature range, two sharp resonances for the acetate group (178.6 and 25.3 ppm) and a 2:1 pattern for

the Me_3Sn ^{13}C resonances are observed at 1.31 and −0.55 ppm, respectively. Even though the Me_3Sn unit in **5** appears rigid at ambient temperature on the time scale of the one-dimensional ^{13}C experiment, the ^{13}C 2D magnetization-transfer experiment reveals the typical reorientational process (see Figure 9). At room temperature the jump rate for **5** is approximately $\kappa = 2.9\ s^{-1}$. With jump rates obtained from eight 2D magnetization-transfer experiments at temperatures between 253 and 324 K (with mixing times τ_m ranging from 90 to 350 ms), the activation energy for the three-site jump in **5** is obtained as $E_a = 68.5 \pm 6.1$ kJ mol^{-1}. The X-ray crystal structure of **5** does not show any unusual bond lengths or bond angles (O–Sn–O bond angle 171.6°; O–Sn distances 220.5 and 239.1 pm; O–Sn–C_{methyl} bond angles between 94.6 (1) and 87.9 (2)°), and in fact these data reflect a fairly good approximation of a regular trigonal bipyramidal Me_3SnO_2 coordination. A somewhat closer look at the structure data, including interactions with neighboring chains in terms of van der Waals interactions, reveals however, that the steric requirements of the $2\pi/3$ jump cannot be accommodated by the structure of **5** quite as easily as is the case for compound **3**, for example.

Compound 6, $(Me_3Sn)_2CO_3$. The polymeric zigzag chain structure of **6** has been described recently, together with some preliminary solid-state NMR results.[17] The main feature of the

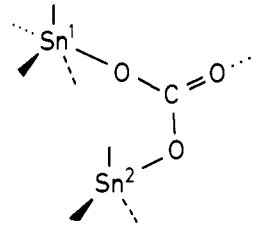

structure of **6** is the simultaneous presence of tetra- and pentacoordinated Me_3Sn groups. Despite the favorable circumstance of a known single crystal X-ray structure of **6**, this compound remains somewhat of a problem case for the following reason. Variable-temperature ^{13}C CP/MAS spectra of **6** clearly show strong temperature dependence,[17] which led us earlier to postulate a $2\pi/3$ jump process as a probable explanation for our experimental observations. In the case of compound **6** the picture could not be refined any further by means of ^{13}C CP/MAS spectroscopy because of overlapping resonances preventing meaningful analysis of one- and two-dimensional ^{13}C experiments in terms of jump rates and activation energies. Still, it is desirable to further characterize at least the mechanism of motion in **6**: in order to exclude motional processes for **6** other than $2\pi/3$ reorientation of the two different Me_3Sn sites, the ^{119}Sn nuclei are available as a probe to gather further circumstantial evidence. Rotor-synchronized ^{119}Sn 2D exchange spectra of **6** show no off-diagonal intensity. But other than for compound **4** (see Figure 8), the two ^{119}Sn spinning sideband patterns for **6** severely overlap on the diagonal. In addition, the signal-to-noise ratio in the ^{119}Sn 2D exchange spectra of **6** is less satisfactory than that for **4** due to insufficient $^1H/^{119}Sn$ CP efficiency for **6** at room temperature. Therefore, this ^{119}Sn 2D exchange spectroscopy result for **6** requires further corroboration. If there was any motion other than $2\pi/3$ jump reorientation, it would certainly be detectable from the tetrahedral Me_3Sn site. To avoid the 2D overlap problem we need to focus on this ^{119}Sn resonance. Tekely et al.[34] have proposed a pulse sequence (SELDOM) which achieves selective excitation of a single resonance by "hard" $\pi/2$ pulses (rather than "soft" pulses in DANTE-type experiments). SELDOM consists of a standard CP experiment to create transverse magnetization, followed by a nonselective $\pi/2$ pulse to align the magnetization along the z-axis. Selective excitation of resonances around the carrier frequency is then achieved by applying the pulse train $[(\pi/2)_x - \tau_1(\text{HPDEC}) - (\pi/2)_{-x} - \tau_2]$ n times (typically $n = 5$ in this case). At the end of each cycle the magnetization is parallel to the z-axis, and a $\pi/2$ pulse converts this into transverse magnetization. The result of such an experiment applied to the ^{119}Sn resonance of the tetrahedral tin atom in **6** is depicted in Figure 10a (using selective excitation, it is then also possible to use sufficiently small spinning

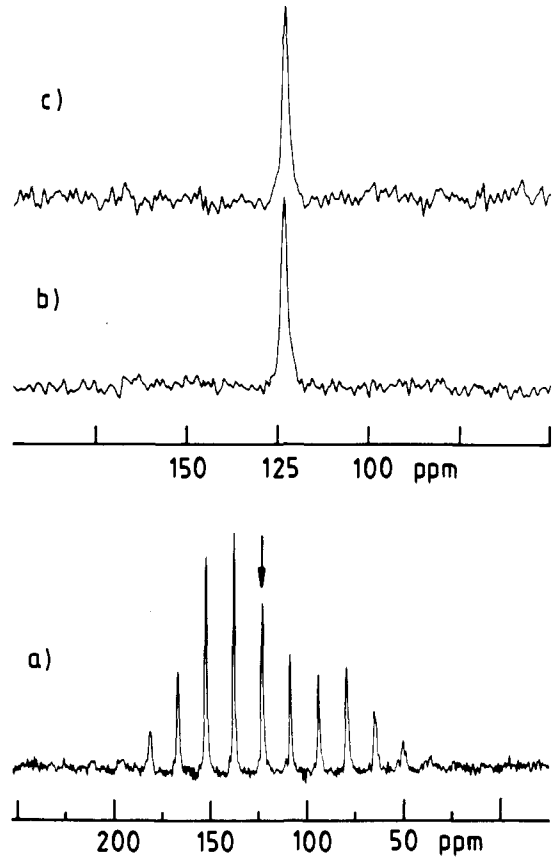

Figure 10. (a) Selective excitation (SELDOM) for the tetrahedral tin site in **6**, $\nu_{rot} = 1620$ Hz, 3149 transients. (b) Selective excitation plus TOSS experiment on the tetrahedral tin site in **6**, $\nu_{rot} = 3462$ Hz, 240 transients. (c) Selective excitation plus TOSS, followed by a mixing time $\tau_m = 6$ s prior to acquisition, $\nu_{rot} = 2462$ Hz, 440 transients.

frequencies which warrant meaningful analysis of the ^{119}Sn csa tensor components of this resonance). An experiment for the detection of motion[35] has been proposed which is based on a TOSS sequence for the elimination of spinning sidebands, followed by a mixing time allowing for the reappearance of spinning sideband intensity in cases where the shielding tensor orientation is time-dependent due to motion or chemical exchange. If we want to use this experiment for our case, i.e., focused on the tetrahedral tin site in **6**, we have to combine the selective excitation SELDOM sequence for the selection of this ^{119}Sn resonance with the TOSS-plus-mixing-time experiment. The results of such a combined experiment are shown in Figures 10b and c. Obviously, no spinning sideband intensity is reintroduced over the mixing time. Given the expressed temperature dependence of all the Me_3Sn–^{13}C resonances of **6**,[17] plus the ^{119}Sn results, we have to conclude that the motional processes in **6** fall into the same category as in **2–5**, both with respect to the mechanism and with respect to activation barriers: the ^{119}Sn one- and two-dimensional experiments show that (i) the backbone of the $(Me_3Sn)_2CO_3$ polymer is rigid apart from the $2\pi/3$ jump reorientation at the trigonal bipyramidal Me_3Sn site and (ii) the only possible reorientation mode for the tetrahedral Me_3Sn site is, again, a $2\pi/3$ jump reorientation.

Discussion

Nonrigidity and reorientational processes in solid transition-metal complexes involving planar, π-bonded organic ligands are fairly well documented and characterized both by spectroscopic methods and by diffraction techniques.[36] Given the fairly moderate activation energies we observe for the Me_3Sn $2\pi/3$ reorientation in **1–6**, one might, therefore, be tempted to ascribe

(35) Yang, Y.; Hagemeyer, A.; Blümich, B.; Spiess, H. W. *Chem. Phys. Lett.* **1988**, *150*, 1–5.
(36) Braga, D. *Chem. Rev.* **1992**, *92*, 633–665.

this process to the presence of a planar Me_3Sn arrangement provided by the trigonal bipyramidal tin coordination in chain polymers like **2–6**. That such a generalization is incorrect is clearly shown by the results for compound **1** where tetrahedral tin is involved in such a 3-site jump process. Just considering the polymeric species **2–6**, one might also be tempted to consider this process as a peculiarity of the Sn–O bond in the solid state. Again, compound **1** proves this statement wrong. Also, qualitative results concerning the internal rotation of Me_3Sn groups in a solid N–Sn–N environment have been reported recently.[37]

Based on our (admittedly still limited) data set, we can nevertheless predict that similar reorientational processes will also be observed for (i) further solid Me_3Sn-containing compounds and (ii) other solid Me_3M compounds with, for example, M = Si, Pb if the respective solid-state structure can accommodate such a process. For simple reasons of space requirements, contradicting the close packing principle, similar processes are most unlikely for solid triorganyltin compounds R_3SnX with ligands R bulkier than R = Me. It should be mentioned, however, that we have also observed nonrigidity for several triphenyltin and triphenyllead compounds[38]—for such compounds no mutual interchange of the phenyl groups has been observed, but smaller-scale motion such as ring wobbles/libration or flips are feasible.

So far, we have shown only that our NMR results do not contradict results from single crystal X-ray diffraction studies. We still need to explore whether, and how well, the kinetic data from NMR spectroscopy will correlate with the picture obtained from X-ray diffraction. In the case of compound **2**, the fairly high activation barrier can be rationalized on the basis of the strongly distorted trigonal bipyramidal Me_3SnO_2 coordination. The deviation of the Me_3Sn plane from perpendicular to the O–Sn–O axis leads to substantial intramolecular (or better, intrachain) van der Waals interactions and thus correlates with a fairly high activation energy for the reorientation of the Me_3Sn group. Compound **5**, $Me_3Sn(O_2CMe)$, also displays a fairly high activation barrier. In contrast to compound **2**, the trigonal bipyramidal environment in **5** is not distorted, and there are no intrachain interactions obstructing the $2\pi/3$ jump. Closer examination of the X-ray crystal structure of **5** reveals that in this case substantial intermolecular, i.e., interchain, van der Waals interactions are responsible for a high activation energy. A rather low activation energy in our series of compounds is determined for compound **3**, and also in this case the single crystal X-ray structure yields direct evidence for (in this case) the ease of Me_3Sn reorientation: the two H_2O molecules act as spacers, leaving room to accommodate this motional process without severe obstruction by van der Waals interactions of the intra- or interchain type. At first glance the low-temperature (178 K) X-ray crystal structure of **4** seems to contradict the low activation energy for Me_3Sn reorientation. The Sn–(OH)–Sn bond angle of 136.9 (1)° causes considerable van der Waals obstruction for the two neighboring Me_3Sn propellers in **4**. At room temperature, however, we observe fairly large—and different—jump rates for the two different Me_3Sn groups. Given the substantial temperature dependence of the ^{119}Sn chemical shift of one of the two tin sites in **4**, we suggest that the Sn–(OH)–Sn bond angle in **4** should increase with increasing temperature, thus lowering the mutual van der Waals interactions between the two Me_3Sn groups and allowing for their independent reorientation. We would also predict then that at sufficiently low temperatures, finally independent reorientation will become impossible and then much slower, correlated reorientation of the two Me_3Sn groups in **4** might occur. Further work along these lines is in progress in our laboratory and will be reported elsewhere.[39]

Acknowledgment. Support of our work by the Deutsche Forschungsgemeinschaft and the Fonds der Chemischen Industrie is gratefully acknowledged. We thank H. Reuter, Universität Bonn, and A. Blaschette and I. Hippel, Technische Universität Braunschweig, for their generous loan of samples **6** and **2–4**, respectively, as well as for making unpublished X-ray diffraction results available to us. We thank S. Gerstmann, Universität Bayreuth, for the preparation of compound **5**. We are most grateful to F. Seifert, Bayerisches Geoinstitut, Bayreuth, for his generous support of our work.

(37) Apperley, D. C.; Davies, N. A.; Harris, R. K.; Eller, S.; Schwarz, P.; Fischer, R. D. *J. Chem. Soc., Chem. Commun.* **1992**, 740–741.
(38) Challoner, R.; Kümmerlen, J.; Sebald, A., to be published.
(39) Blaschette, A.; Hippel, I.; Kümmerlen, J.; Sebald, A., to be published.

Communications to the Editor

A New Family of Icosahedral Cages with Transition Metal and Main Group IV (14) Atoms: Synthesis and Structural-Bonding Analysis of the $[Ni_{11}(SnR)_2(CO)_{18}]^{2-}$ Dianions (R = *n*-Bu, Me) Containing Ni-Centered Icosahedral $Ni_{10}Sn_2$ Cages and of Their Unusual $[Ni(SnRCl_2)_4(CO)]^{2-}$ Precursors Containing a Trigonal-Bipyramidal d^8 Nickel(II) Configuration

Jeffrey P. Zebrowski,[1] Randy K. Hayashi, and Lawrence F. Dahl*

Department of Chemistry
University of Wisconsin—Madison
Madison, Wisconsin 53706

Received September 10, 1991

Reactions in our laboratory of $[Ni_6(CO)_{12}]^{2-}$ (**1**)[2] with organo(main group V (15)) dihalides have given rise to a variety of clusters, including ones with discrete noncentered metal(main group) icosahedral cages.[3] Such 12-atom clusters, which are electronically equivalent (i.e., 13 skeletal electron pairs) with the classic $[B_{12}H_{12}]^{2-}$ dianion[4] and $[Al_{12}R_{12}]^{2-}$ (R = *i*-Bu),[5] include members of the $[Ni_{12-x}(PMe)_x(CO)_{24-3x}]^{2-}$ (x = 2–4)[6] and $[Ni_{12-x}(AsR)_x(CO)_{24-3x}]^{2-}$ (x = 2, R = Me; x = 3, R = Ph)[7] series

(1) Current address: Argonne National Laboratory, Chemical Technology Division, 9700 South Cass Avenue, Argonne, IL 60439.

(2) (a) Calabrese, J. C.; Dahl, L. F.; Cavalieri, A.; Chini, P.; Longoni, G.; Martinengo, S. *J. Am. Chem. Soc.* **1974**, *96*, 2616–2618. (b) Longoni, G.; Chini, P.; Cavalieri, A. *Inorg. Chem.* **1976**, *15*, 3025–3029.
(3) (a) DesEnfants, II, R. E.; Gavney, J. A., Jr.; Hayashi, R. K.; Rae, A. D.; Dahl, L. F.; Bjarnason, A. *J. Organomet. Chem.* **1990**, *383*, 543–572 and references therein. (b) Mlynek, P. D.; Dahl, L. F. Unpublished research.
(4) (a) Lipscomb, W. N.; Wunderlich, J. A. *J. Am. Chem. Soc.* **1960**, *82*, 4427–4428. (b) Pitochelli, A. R.; Hawthorne, M. F. *J. Am. Chem. Soc.* **1960**, *82*, 3228–3229. (c) Meutterties, E. L.; Merrifield, R. E.; Miller, H. C.; Knoth, Jr., W. H.; Downing, J. R. *J. Am. Chem. Soc.* **1962**, *84*, 2506–2508.
(5) Hiller, W.; Klinkhammer, K.-W.; Uhl, W.; Wagner, J. *Angew. Chem., Int. Ed. Engl.* **1991**, *30*, 179–180.
(6) (a) Rieck, D. F.; Rae, A. D.; Dahl, L. F. *Abstracts of Papers*, 190th National Meeting of the American Chemical Society, Chicago, IL, Sept. 1985; American Chemical Society: Washington, D.C., 1985; INOR 157. (b) Rieck, D. F.; Gavney, J. A., Jr.; Norman, R. L.; Hayashi, R. K.; Dahl, L. F. *J. Am. Chem. Soc.* **1992**, *114*, 10369–10379.

0002-7863/93/1515-1142$04.00/0